The Cryosphere Open Access
Discussions

Initial results from geophysical surveys and shallow coring of the Northeast Greenland Ice Stream (NEGIS)

P. Vallelonga[1], K. Christianson[2,3], R. B. Alley[4], S. Anandakrishnan[4],
J. E. M. Christian[3], D. Dahl-Jensen[1], V. Gkinis[1], C. Holme[1], R. W. Jacobel[3],
N. Karlsson[1], B. A. Keisling[3,5], S. Kipfstuhl[6], H. A. Kjær[1], M. E. L. Kristensen[1],
A. Muto[4], L. E. Peters[4], T. Popp[1], K. L. Riverman[4], A. M. Svensson[1], C. Tibuleac[1],
B. M. Vinther[1], Y. Weng[1], and M. Winstrup[1]

[1]Centre for Ice and Climate, Niels Bohr Institute, University of Copenhagen, Juliane Maries vej
30, Copenhagen 2100, Denmark
[2]Courant Institute of Mathematical Science, New York University, 251 Mercer St, New York,
NY 10012, USA
[3]Physics Department, St Olaf College, 1520 St Olaf Ave, Northfield, MN 55057, USA
[4]Department of Geosciences and Earth and Environmental Systems Institute, The
Pennsylvania State, University Park, PA 16802-6813, USA
[5]Department of Geosciences, University of Massachusetts Amherst, 611 North Pleasant
Street, Amherst, MA 01003-9297, USA
[6]Alfred Wegener Institute, Am Handelshafen 12, 27570 Bremerhaven, Germany

TCD

8, 691–719, 2014

Initial results from Northeast Greenland Ice Stream (NEGIS)

P. Vallelonga et al.

Title Page

Abstract	Introduction
Conclusions	References
Tables	Figures

Back | Close

Full Screen / Esc

Printer-friendly Version

Interactive Discussion

Initial results from Northeast Greenland Ice Stream (NEGIS)

P. Vallelonga et al.

Title Page

Abstract	Introduction
Conclusions	References
Tables	Figures

Back   Close

Full Screen / Esc

Printer-friendly Version

Interactive Discussion

Abstract

The Northeast Greenland Ice Stream (NEGIS) is the sole interior Greenlandic ice stream. Fast flow initiates near the summit dome, and the ice stream terminates approximately 1000 km downstream in three large outlet glaciers that calve into the Greenland Sea. To better understand this important system, in the summer of 2012 we drilled a 67 m firn core and conducted ground-based radio-echo sounding (RES) and active-source seismic surveys at a site approximately 150 km downstream from the onset of streaming flow (NEGIS firn core, 75°37.61′ N, 35°56.49′ W). The site is representative of the upper part of the ice stream, while also being in a crevasse-free area for safe surface operations.

Annual cycles were observed for insoluble dust, sodium and ammonium concentrations and for electrolytic conductivity, allowing a seasonally resolved chronology covering the past 400 yr. Annual layer thicknesses averaged 0.11 m ice equivalent (i.e.) for the period 1607–2011, although accumulation varied between 0.08 and 0.14 m i.e., likely due to flow-related changes in surface topography. Tracing of RES layers from the NGRIP ice core site shows that the ice at NEGIS preserves a climatic record of at least the past 51 kyr. We demonstrate that a deep ice core drilling in this location can provide a reliable Holocene and late-glacial climate record, as well as helping to constrain the past dynamics and ice-lithosphere interactions of the Greenland Ice Sheet.

1 Introduction

Mass loss of the Greenland Ice Sheet (GIS) is accelerating (Rignot et al., 2011). Although the multiple processes involved are not fully understood (Wouters et al., 2013), approximately 50 % of net Greenland mass loss has been attributed to increased ice stream discharge, with other mass loss mechanisms including changing patterns of surface accumulation and runoff (van den Broeke et al., 2009). The mechanisms governing ice stream discharge are complicated, and include bedrock conditions as well

as buttressing effects at the ice sheet margin. Changes in basal processes are difficult to monitor directly, but may have contributed to enhanced ice stream discharge. Faster ice flow may have increased frictional heating and thus basal melting of grounded ice, which is usually neglected in mass-balance estimates (van den Broeke et al., 2009)
5 but may be locally significant.

A growing concern is the potential for additional rapid changes in ice dynamics that could contribute to further acceleration of mass loss. While the buttressing effect of floating glacier tongues (Moon et al., 2012) and the immediate effect of the melting of submarine ice tongues (Holland et al., 2008) have been widely studied, bedrock
10 topography frequently limits the inland propagation of such effects, and glaciers may reset their flow rates to accommodate new geometries with upstream mass loss limited to diffusive processes and their subsequent effects on surface mass balance (Bamber et al., 2013; Joughin et al., 2012b). Thus, current GIS mass loss due to ice-ocean interactions may be limited ($\sim 3\times$ current mass loss rates for Jakobshavn Isbræ, Pfeffer
15 et al., 2008), and many outlet glaciers will eventually stabilize once they encounter bed sills or withdraw from fjord troughs (Joughin et al., 2012a; Joughin et al., 2012b).

An unknown in estimates of past and future mass loss of GIS is the behaviour of the northern Greenland Ice Sheet, where Atlantic Water (AW) reaching grounding lines currently remains relatively cold (0–1 °C; Straneo et al., 2012), but may warm by several
20 degrees in the next 100 yr (Yin, 2012). Of principal importance are Petermann Glacier (80°45′ N, 60°45′ W), and the Northeast Greenland Ice Stream (NEGIS), whose great inland extent may facilitate especially rapid inland respond to ocean-induced coastal thinning (Figs. 1 and 2).

NEGIS is the largest ice stream in Greenland and is the only ice stream that extends
25 far inland (Fahnestock et al., 1993; Fahnestock et al., 2001; Joughin et al., 2001). The onset of streaming flow is at the central ice divide, and the ice stream terminates in three large outlet glaciers (Nioghalvfjerds isstrømmen, Zachariae isbræ and Storstrømmen) approximately 1000 km downstream (Figs. 1 and 2). NEGIS was first identified in 1993 using synthetic aperture radar (SAR) imagery (Fahnestock et al., 1993), with sub-

sequent studies of bedrock topography and satellite radar interferometry (SRI) allowing evaluations of the velocity, mass balance, and basal characteristics of the ice stream (Fahnestock et al., 2001). The onset of the ice stream on the ice divide is likely caused by strong basal melt due to regionally high geothermal flux (Fahnestock et al., 2001; Petrunin et al., 2013), which results in enhanced lubrication and fast flow. The downstream acceleration of the ice stream (to 100 m yr^{-1} approximately 200 km downstream from the ice divide) is likely the result of basal water routing via ice dynamic feedbacks and the presence of subglacial till, which will deform if sufficient pressurized subglacial water is present (Christianson et al., 2014). The past and present behaviour of NEGIS and its effect on the behaviour of the Greenland Ice Sheet, such as the inland effects of recent modest coastal acceleration following breakup of an ice shelf (Joughin et al., 2010), are poorly known due to sparse data and the relatively recent discovery of the ice stream (Fahnestock et al., 1993).

The majority of Greenland deep ice core drillings have occurred along the central ice divide (Fig. 1), with the aim of accessing the oldest ice strata, whereas there have been few ice core-based studies of Northeast Greenland due to its inaccessibility and more complex ice dynamics. The NorthGRIP (NGRIP) deep drilling program produced a 3085 m long ice core (NGRIP members, 2004), obtaining a continuous, well-preserved record of climate and impurities for the past 123 kyr. The ice core chronology obtained from NGRIP (Wolff et al., 2010) can be used to date radio-echo sounding (RES) layers at the NEGIS shallow core site (75°37.61′ N, 35°56.49′ W; Figs. 1 and 2) via tracing of continuous internal layers visible in airborne and ground-based RES data. Records of snow accumulation and deposition of sulfate and nitrate in Northeast Greenland are available from firn and ice cores drilled during the 1993–1995 North Greenland Traverse (NGT) program (Fischer et al., 1998b). The NGT results demonstrate consistently lower snow accumulation rates to the east than to the west of the Greenland ice divide, and also highlight anthropogenic sulfate and nitrate production during the 20th century (Fischer et al., 1998a; Bigler et al., 2002). A 1200-year record of sulfate, calcium, and sodium at the B20 site (78°50′ N, 36°30′ W; 2150 m a.s.l.) in North-

east Greenland also demonstrated regular annual layer thicknesses of approximately 10 cm water equivalent (Bigler et al., 2002). The B20 core chronology was established primarily by the identification of volcanic deposition strata, although annual cycles in sulphate, calcium, and sodium were also detected and counted with a chronological
5 uncertainty of ±5 yr between volcanic strata.

Here we present a detailed geophysical and glaciochemical study of the upstream section of NEGIS, concentrating on reconstructing recent climate history and using newly acquired knowledge of ice dynamics to place this history in context. The geophysical data allow evaluations of the basal characteristics and flow dynamics of the ice
10 stream, whereas the glaciochemical data allow past surface accumulation and impurity deposition to be reconstructed for the site. These data allow an improved estimate of the potential age of stratigraphically coherent ice layers that can be obtained from Northeast Greenland. Furthermore, these findings are necessary for an improved understanding of the processes contributing to ice stream formation and dynamics as well
15 as ice-lithosphere interactions. Our study also aids in the assessment of the stability of Greenland's only inland ice stream. This work indicates that additional field studies are necessary to understand the past and future behaviour of NEGIS, including its effect on ice sheet mass balance and sea level.

2 Methods

2.1 Firn core drill site

In June 2012, a 67 m firn core was drilled at the NEGIS borehole site (75.623° N 35.96° W, Figs. 1–3). At the site, the ice flows $\sim 60\,\mathrm{m\,yr^{-1}}$ horizontally to the northeast. The core was drilled in a dry borehole using a 3″ diameter electromechanical drill. The firn core was cut into 55 cm bag lengths at the drill site and then packed for
25 transport to the NEEM deep ice core drilling camp, where DiElectric Profiling (DEP) analysis (Moore et al., 1989) was conducted.

2.2 Surface geophysical surveys

We collected ∼ 350 line kilometres of kinematic GPS and RES data, five wide-angle seismic profiles, and five shallow refraction profiles in summer 2012, sampling areas of streaming flow and of adjacent slow moving ice (Fig. 3). GPS data were processed using differential carrier-phase positioning (Chen, 1998) relative to a fixed nearby base station. RES data were collected using a monopulse system operating at a centre frequency of ∼ 3 MHz (Welch and Jacobel, 2003; Welch et al., 2009). RES data processing included bandpass filtering, correction for antenna spacing, interpolation to standard trace spacing, two-dimensional migration, and correction for spherical divergence and englacial attenuation (Christianson et al., 2012). Grids of surface and bed elevation (relative to WGS84 ellipsoid) were interpolated using the nearest-neighbour algorithm, where bed elevation was calculated assuming a uniform radar wave speed in ice of 169 m µs^{-1} (Fig. 3). At each seismic site (labelled A-E in Fig. 3), explosive sources and receivers were positioned to sample the same 480 m section of the bed over a continuous source-to-receiver offset of 0 to 4800 m (approximately 0–45° incidence angle). Amplitude-vs.-offset (AVO) analysis of the ice bottom reflection (Peters et al., 2007, 2008; Peters, 2009; Aki and Richards, 2002) was performed to constrain elastic properties of the basal material. Shallow refraction profiles were processed for firn depth and density following Kirchner and Bentley (1990) and Kohnen (1972), respectively. Further details on geophysical data collection and processing are presented in Christianson et al. (2014).

2.3 CFA analysis

In January 2013, the NEGIS firn core was analysed using the Continuous Flow Analysis (CFA) system developed at CIC for high-resolution analysis of ice cores. Density measurements and Electrical Conductivity Measurements (ECM) were conducted prior to cutting a 35 mm × 35 mm longitudinal section for CFA (Kjær et al., 2013). The CFA system allows the continuous determination of impurities, such as sodium (Na$^+$), am-

monium (NH_4^+), insoluble dust particles and electrolytic conductivity (Bigler et al., 2011) as well as stable water isotope ratios (Gkinis et al., 2011). The upper 20 m of the core was melted at a rate of 5 cm min^{-1}, while the denser firn section was melted at a rate of 4 cm min^{-1}. Blanks and calibration standards were determined at the start, middle, and end of each day of analysis, during which approximately 7 m of firn was melted.

2.4 Water stable isotope analysis

The firn core was cut into 5 cm samples for stable isotope analysis, with two surface snow pits also analysed. Thus, a total of 1325 discrete samples were collected from the surface down to 66.3 m, with a sampling resolution of 5 cm. The samples were melted in dry airtight metal containers and stored in 5 mL plastic containers. 1.5 mL of each melted sample was pipetted into a 2 mL vial stored in a refrigerator to avoid evaporation between sampling and measurement. Each measurement run consisted of 3 standards and 39 discrete samples. To minimize the memory effect, each standard was injected 12 times and only the last 5 injections were used. Each discrete sample was injected 4 times and only the last 3 injections were used.

The samples were measured on a Picarro L2120-i Near Infrared Cavity Ring Down Spectrometer (IR-CRDS) using the high throughput Picarro-A0212 vaporizer (Gkinis et al., 2010). The latter is superior to the more standard high precision Picarro-A0211 vaporizer regarding memory effects. Considering the dependence of the IR-CRDS system on humidity levels, the water concentration was kept between 19 000–20 500 ppmv (parts per million by volume) during analyses. Results are reported with respect to Vienna Standard Mean Ocean Water (VSMOW) and normalized to the VSMOW – SLAP (Standard Light Antarctic Precipitation) scale using $\delta^{18}O_{VSMOW} = 0.0‰$, $\delta^{18}O_{SLAP} = -55.5‰$, $\delta D_{VSMOW} = 0.0‰$ and $\delta D_{SLAP} = 427.5‰$. Note that this approach implies the use of a fixed two-point calibration line. We used 3 in-house standards with well-calibrated $\delta^{18}O$ and δD values with respect to the primary IAEA standard waters. Two of the in-house standards are used for the estimation of the two-point calibration line

and the third serves as a quality control. The overall precision of the system was determined to be better than 0.1‰ for δ^{18}O and 0.5‰ for δD.

2.5 Core chronology and annual layer counting techniques

The NEGIS core chronology was established using the common technique of identifying volcanic deposition strata and then counting of annual layers determined from CFA measurements. For the top 3 m of the core, annual layer counting was based on the discrete δ^{18}O annual cycles because the compacted snow was not suitable for CFA analysis. Volcanic strata were identified by DEP and confirmed using ECM and electrolytic conductivity measurements (Kjær et al., 2013). The main volcanic strata identified included: Katmai (1912), Tambora (1816), Unknown (1810), Laki (1783), and Komagatake (1640). Annual layers between volcanic strata were counted using two independent methods: a manual approach (Andersen et al., 2006) and an automated algorithm (Winstrup et al., 2012). The manual and algorithmic layer counting techniques were in agreement for all of the NEGIS record and confirmed the volcano-based estimate. Thus, we can determine the NEGIS core chronology to be accurate with a precision of ±1 yr for the past ∼ 400 yr. The age at the bottom of the core is 1607 ± 1 AD. The annual layer thickness (λ) was derived from the layer counting.

To extend the chronology of the NEGIS drill site beyond 1607, we used the NGRIP ice core chronology (Wolff et al., 2010) to date internal layers in airborne RES data connecting the NEGIS and NGRIP drill sites (Keisling et al., 2014). Internal layers were identified in and propagated through RES profiles using a semi-automatic algorithm that identifies the peak of the radar wavelet nearest an initial user-identified peak, then automatically selects the flanking changes in concavity, and finally follows this wavelet along a radar profile. As occasional user interaction is required, two independent interpreters informed the layer-tracing algorithm to eliminate user bias. We were able to identify 27 internal layers at NGRIP; 14 of these layers were continuous in airborne RES profiles between NGRIP and NEGIS (Keisling et al., 2014). Although the deepest continuous layer traceable from NGRIP to NEGIS is only ∼ 51 ka, there is ∼ 600 m of

Title Page

Abstract | Introduction

Conclusions | References

Tables | Figures

|◀ | ▶|

◀ | ▶

Back | Close

Full Screen / Esc

Printer-friendly Version

Interactive Discussion

additional ice present at NEGIS with many additional coherent internal layers present (Fig. 4; Keisling et al., 2014). Thus the ice here is likely to be considerably older than ∼ 51 ka. Although the uncertainty in this layer-tracing approach is significant, and increases with depth due to increasing uncertainty in both layer age and depth calcu-

5 lations, the uncertainty in the deepest layers is on the order of only a few thousand years. Internal layers in the deepest ice (0–300 m above the bed) are blurry, and although there are traceable packets of energy, clear radar wavelets similar to a Ricker wavelet are not present. It is possible that stratigraphy in this deepest ice has been disturbed due to ice folding and overturning in a similar manner to ice in the deepest

10 sections of the NEEM ice core (NEEM Community members, 2013).

3 Results

3.1 Chemistry

The NEGIS impurity record shows stable values for all parameters over the past 400 yr, with the exception of conductivity, which varies during the second half of the 20th cen-

15 tury (Fig. 5). Sodium is derived from sea salt inputs, and exhibits a regular peak in winter, likely due to increased winter storminess (Legrand and Mayewski, 1997). Mineral dust particles are transported to Greenland primarily in the spring/summer period, and have been geochemically linked to the Gobi and Taklamakan Deserts in central Asia (Bory et al., 2003). No centennial-scale trends were observed in sodium or dust

20 particles. Ammonium, originating from biogenic sources such as biomass burning, bacterial decomposition and soil emissions (Legrand et al., 1992), peaks in the summer, when temperatures are highest. The NEGIS record shows relatively few large ammonium peaks during the 20th century, which is consistent with other studies observing a decrease in large-scale boreal forest fires as a result of changes in grazing, agricul-

25 ture and fire management practices (Marlon et al., 2008). The electrolytic conductivity, which indicates the total ionic impurity loading in the ice, is elevated between 1950 and

2000 and peaks during the 1970s. The results agree with similar trends of sulfate and nitrate concentrations observed in the North Greenland traverse cores, and attributed to industrial emissions from Europe and North America (Fischer et al., 1998b).

3.2 Isotopes

The isotopic composition is strongly smoothed by diffusion. The layer counting based on the discrete $\delta^{18}O$ annual cycles is available for only the top ~ 7 m of the core. Due to the difference between diffusion velocities of $\delta^{18}O$ and δD, deuterium excess shows clear annual cycles until ~ 10 m depth. The $\delta^{18}O$ profile shows relatively light values from roughly 30–45 m (Fig. 5), where the annual layer thickness is greater than sections immediately above and below (Fig. 6). This feature of the profiles of $\delta^{18}O$ and annual layer thickness was likely generated by the effect of upstream topographic undulations on accumulation, and advected to the core site by ice flow (Figs. 2 and 3; Reeh et al., 1985).

3.3 Surface geophysical surveys

3.3.1 Surface topography

Our focused survey and earlier regional analyses (Joughin et al., 2001; Fahnestock et al., 2001) show that streaming flow and a broad surface depression are spatially coincident (Figs. 2a and 3), although as discussed next, there is important topography within this broad surface depression correlated with features of the ice stream. Within the ice stream, elevation generally decreases from the ice sheet summit towards the coast, but there are numerous localized areas where elevation increases along-flow (Fig. 2a). The most distinct surface expression of NEGIS is the presence of well-defined troughs along the shear margins (Fig. 2; Fahnestock et al., 2001; Joughin et al., 2001). Unlike other ice streams, which have well-developed tributary systems (Rignot et al., 2011), streaming flow in NEGIS is primarily supplied by ice that passes through a shear

margin (Fig. 2c). The downstream widening reduces lateral drag on the ice after it has flowed through a shear margin, allowing strong velocity increase along-flow that favours surface thinning and a local low in surface elevation and basal hydropotential, in turn driving basal water routing roughly downstream and along-flow (Christianson et al.,
5   2014).

3.3.2   Bed topography

Unlike most other ice streams, the region of fastest flow is not underlain by a prominent basal topographic trough (Figs. 2b and 3). The fastest flow in our survey region is actually over the area of highest bed elevation. The prominent surface troughs that
10   mark the shear margins do not closely mirror bed topography; the northwest shear margin does somewhat overlie a shallow trough beneath, but the narrow basal trough on the southeast side runs approximately $-15°$ off-axis and terminates directly downstream of our ground-based survey (Figs. 2b and 3). Hydropotential is highest in the central portion of the ice stream, consistent with subglacial water flowing downstream
15   and spreading as the ice stream widens, allowing enhanced lubrication and flow. Basal water routing along the shear margins is complex, and is further discussed in Christianson et al. (2014). In contrast to West Antarctic ice streams (Bell et al., 1998; Bingham et al., 2012), bed topography is not a primary control on the inland part of streaming flow in northeast Greenland. This agrees with other recent compilations of Greenland
20   bed topography (Bamber et al., 2013b; Fig. 2b), which show that prominent features in bed topography do not control current ice flow direction in northern Greenland.

3.3.3   Basal lithology

Seismic AVO analysis allows us to determine elastic properties of the basal material (density, compressional-wave velocity, and shear-wave velocity), which, in turn, can
25   be interpreted as an indicator of likely basal material. Our AVO analysis (Christianson et al., 2014) indicates that dilatant till (~ 10 m thick) is present at site C, near the

firn core site in the central part of the ice stream (Fig. 3). The subglacial sediment is somewhat more consolidated at sites B and D, one in each shear margin, with well-consolidated sediment at sites A and E outboard of the shear margins (Fig. 3). The pattern of radar basal reflectivity (Christianson et al., 2014) and hydropotential sup-
⁵ ports and extends the seismic data. The radar data indicate that the central portion of the ice stream bed is wet, with water flow generally oriented along-flow. A hydropotential low beneath the surface trough of each shear margin acts as a barrier to both ingress and egress of subglacial water. These data suggest that streaming flow is due to basal lubrication caused by deforming sediment and high-pressure water in a man-
¹⁰ ner similar to that seen on Siple Coast ice streams in West Antarctica (Peters et al., 2007, 2008; Blankenship et al., 1986; Alley et al., 1986; Kamb, 2001). The occurrence of sediment outside of streaming flow (sites A and E) suggests that streaming flow could shift location and possibly expand in response to redirection of subglacial water.

Our seismic and radar surveys were designed to image the basal interface of NEGIS,
¹⁵ rather than deeper geologic structures. Therefore, we cannot map the amplitude or spatial extent of the geothermal flux anomaly under portions of the ice stream, nor can we assess the presence or absence of a sedimentary basin under NEGIS similar to that under some West Antarctic ice streams (Anandakrishnan et al., 1998). Thus, additional field data are needed to understand the crustal structure of Northeast Greenland and
²⁰ its effect on ice sheet behaviour.

3.3.4 Firn characteristics

Ice density profiles derived from seismic shallow refraction data (Christianson et al., 2014) indicate that firn densification rates are significantly greater in the ice stream margins than in the central portions of the ice stream and outside of streaming flow
²⁵ (Fig. 7). As discussed by Alley and Bentley (1988) firn densification includes power-law-creep processes dependent on the second invariant of the stress tensor, especially for densities higher than $\sim 550\,\mathrm{kg\,m^{-3}}$. Thus, densification is accelerated by the ice flow stresses that cause surface strain rates. The high stresses causing the rapid side

shear in the shear margins also produce faster firn densification rates. We estimate from the seismic data that there is as much as 20 m of additional ice in the shear margins compared to outside the ice stream for the same total thickness of firn and ice. This observation is significant for two reasons: (1) ice thickness and hydropotential are frequently calculated assuming a constant firn thickness of uniform density or no firn correction and (2) an ice core drilled in a shear margin or through a past shear margin will exhibit variations in density profiles and possibly crystal orientation fabric (COF).

The surface troughs associated with the shear margins capture drifting snow, thereby increasing accumulation. Based on measured surface strain rates, Fahnestock et al. (2001) calculated that the maximum trough depth would be more than 200 m, much more than observed, and suggested that enhanced accumulation in the troughs explains this difference, with implied rates in excess of $1\,\mathrm{m\,yr^{-1}}$ of ice in this high, cold location. Our radar is designed primarily for sounding the full ice thickness and thus cannot see individual annual layers to trace their thickness change through the shear margins, but variations in depth of the shallowest layer (300 m depth) fully support the inference of anomalously high accumulation in the shear margins (km 8–15; km 33–36 in Fig. 4). From the observed velocity vectors, we calculate that the firn core consists entirely of accumulation from within the ice stream, and so is not affected by the accumulation anomalies of the troughs.

4 Discussion

4.1 NEGIS accumulation profile

The annual layer thickness profile determined for the NEGIS firn core demonstrates a reliable accumulation history for the past 400 yr ($\sim 0.11\,\mathrm{m}$ i.e. $\mathrm{yr^{-1}}$). Although annual layer thicknesses (Fig. 6) vary gradually through the profile, the number of counted years corresponds well to volcanic tiepoints, confirming that remobilization of surface snow is unlikely at the NEGIS site.

Sufficiently rapid ice flow over bed topography or variations in basal lubrication causes surface topography, in turn producing variations in accumulation rate from trapping of drift snow (e.g., Gow, 1965, for near Byrd Station, Antarctica; also see Reeh et al., 1985). Thus, any ice core sufficiently far downstream is expected to exhibit accu-
5 mulation variations. As shown in Fig. 3, surface undulations are present in the vicinity of the NEGIS drill site (also see Fahnestock et al., 2001), so we expect accumulation-rate variations in NEGIS ice cores. Figure 6 compares annual layer thickness profiles for NEGIS and the uppermost 70 m of the NGRIP ice core. Compared to the NGRIP profile, it is apparent that NEGIS annual layer thicknesses are anomalously low at two
10 depth ranges, at ∼ 20 m and from ∼ 50 to ∼ 60 m depth. The ice-equivalent annual layer thickness decreases from an average value of 0.12 ± 0.02 m i.e. (1σ error, 30–40 m depth) to 0.09 ± 0.01 m i.e. (1σ error, 50–60 m depth), most likely due to advection of accumulation rate variability from an upstream area of enhanced surface topography.

The stable shear margins (Fahnestock et al., 2001), with their very large effects on
15 firn densification and snow accumulation rate, offer a unique laboratory for additional studies. The great range of strain rates and accumulation rates, with somewhat different conditions in the two shear margins, at nearly the same temperature, should allow assessment of the role of different densification mechanisms (linear-viscous vs. power-law creep; e.g., Alley, 1987), and thus could lead to improved firn-densification
20 modeling, which is of great value in ice core studies as well as for the overall projection of ice sheet models and reconstruction of past ice sheet flow. The anomalously enhanced accumulation rate in the shear margins may be the highest value that can be reliably sampled at such a low temperature. This suggests a useful target for studies requiring large volumes of ice, especially from recent times when identification of the
25 anomaly is especially easy.

4.2 NEGIS flow history and bedrock characteristics

The lack of a topographic trough under the ice stream suggests that NEGIS is especially sensitive to subglacial water routing and feedbacks between ice thickness and

subglacial erosion that influence hydropotential. Christianson et al. (2014) suggest the following extended hypothesis: a small region of high geothermal flux near the ice-divide produces a plume of subglacial lubricating meltwater, giving NEGIS an inland origin. The plume spreads downstream in response to flow around basal obstacles in the absence of a strongly channelizing hydropotential gradient distribution, and this spreading, likely aided by ice flow processes, causes the ice stream to widen downstream (Alley and Whillans, 1991). Thus, streaming flow is supplied almost entirely by ice that passes through a shear-margin. The downstream widening reduces the lateral drag on ice after it has flowed through the shear-margin, allowing strong velocity increase along-flow that favors surface thinning and a local low in surface elevation and basal hydropotential. The resulting focusing of lubricating water leaves bands of poorly lubricated bed as part of the shear-margin complex, restricting ice and water flow into the ice stream. Therefore, inland ice does not form a broad catchment tightly coupled to marginal changes.

Sufficiently large thinning along the ice stream from coastal forcing of the three outlet glaciers might remove the surface troughs and their effects, allowing NEGIS to tap a larger catchment area. This possibility, plus a host of questions, such as the sources and transport of till, and whether the ice stream can have persisted over long times without eroding a trough, motivate additional observations and modeling. Additional seismic and radar data would aid in crustal structure mapping and determination of ice-lithosphere interaction in the vicinity of NEGIS. Additional data on past climate are also needed to allow proper incorporation of NEGIS into ice sheet models that will allow accurate past and future simulations of the Greenland Ice Sheet. The proximity of NEGIS to zones of deep water formation in the Greenland Sea, and ability of NEGIS to rapidly discharge large amounts of ice, suggest it may have a unique ability to influence the southward transport of surface waters from the Greenland Sea, and ultimately Atlantic meridional ocean circulation. Thus, understanding the past and future behavior is important not only to predict future sea level contributions, but also to understand past rapid changes in climate.

5   Conclusions

We conducted an integrated geophysical and glaciochemical study on the Northeast Greenland Ice Stream, focusing on an area approximately 150 km east of the NGRIP ice core drilling site. The data presented here indicate that the NEGIS site retains a reliable, annually-resolved record of chemical impurities including sodium, ammonium and mineral dust. A 67 m firn core drilled at the site was dated back to 1607 AD, by a combination of annual layer counting as well as volcanic tiepoints. The surface accumulation has been relatively stable over the past 400 yr, although some variability has been observed in surface accumulation, due to upstream ice flow variability inducing irregular surface topography. Tracking of RES layers from NGRIP to the NEGIS site indicates that the NEGIS site preserves a stratigraphically intact climate archive of at least 51 kyr duration. The character of the shear margins offers an outstanding opportunity to improve understanding of firn densification, and to find recent samples with exceptionally high accumulation rate at such a low temperature. Deeper ice may contain information on past changes or ongoing processes in ice stream dynamics that are important to understand in order to properly incorporate NEGIS into models of the Greenland Ice Sheet, which is necessary to accurately forecast and hindcast ice sheet geometry and dynamics with their accompanying climatic ramifications.

References

Aki, K. and Richards, P. G.: Quantitative Seismology, 2 edn., University Science Books, Sausalito, 2002.

Alley, R. B., Blankenship, D. D., Bentley, C. R., and Rooney, S. T.: Deformation of till beneath Ice Stream B, West Antarctica, Nature, 322, 57–59, doi:10.1038/322057a0, 1986.

Alley, R. B.: Firn densification by grain-boundary sliding: a first model, J. Phys.-Paris, 48, 249–254, doi:10.1051/jphyscol:1987135, 1987.

Alley, R. B. and Bentley, C. R.: Ice-core analysis on the Siple Coast of West Antarctica, Ann. Glaciol., 11, 1–7, 1988.

Alley, R. B. and Whillans, I. M.: Changes in the West Antarctic ice sheet, Science, 254, 959–963, doi:10.1126/science.254.5034.959, 1991.

Anandakrishnan, S., Blankenship, D. D., Alley, R. B., and Stoffa, P. L.: Influence of subglacial geology on the position of a West Antarctic ice stream from seismic observations, Nature, 394, 62–65, doi:10.1038/27889, 1998.

Andersen, K. K., Svensson, A., Rasmussen, S. O., Steffensen, J. P., Johnsen, S. J., Bigler, M., Röthlisberger, R., Ruth, U., Siggaard-Andersen, M.-L., Dahl-Jensen, D., Vinther, B. M., and Clausen, H. B.: The Greenland Ice Core Chronology 2005, 15–42 ka, Part 1: constructing the time scale, Quaternary Sci. Rev., 25, 3246–3257, doi:10.1016/j.quascirev.2006.08.002, 2006.

Bamber, J. L., Griggs, J. A., Hurkmans, R. T. W. L., Dowdeswell, J. A., Gogineni, S. P., Howat, I., Mouginot, J., Paden, J., Palmer, S., Rignot, E., and Steinhage, D.: A new bed elevation dataset for Greenland, The Cryosphere, 7, 499–510, doi:10.5194/tc-7-499-2013, 2013.

Bell, R. E., Blankenship, D. D., Finn, C. A., Morse, D. L., Scambos, T. A., Brozena, J. M., and Hodge, S. M.: Influence of subglacial geology on the onset of a West Antarctic ice stream from aerogeophysical observations, Nature, 394, 58–61, doi:10.1038/27883, 1998.

Bigler, M., Wagenbach, D., Fischer, H., Kipfstuhl, J., Miller, H., Sommer, S., and Stauffer, B.: Sulphate record from a northeast Greenland ice core over the last 1200 years based on continuous flow analysis, Ann. Glaciol., 35, 250–256, doi:10.3189/172756402781817158, 2002.

Bigler, M., Svensson, A., Kettner, E., Vallelonga, P., Nielsen, M., and Steffensen, J. P.: Optimization of high-resolution continuous flow analysis for transient climate signals in ice cores, Environ. Sci. Technol., 45, 4483–4489, doi:10.1021/es200118j, 2011.

Bingham, R. G., Ferraccioli, F., King, E. C., Larter, R. D., Pritchard, H. D., Smith, A. M., and Vaughan, D. G.: Inland thinning of West Antarctic Ice Sheet steered along subglacial rifts, Nature, 487, 468–471, doi:10.1038/nature11292, 2012.

Initial results from Northeast Greenland Ice Stream (NEGIS)

P. Vallelonga et al.

Title Page

Abstract | Introduction

Conclusions | References

Tables | Figures

◀◀ | ▶▶

◀ | ▶

Back | Close

Full Screen / Esc

Printer-friendly Version

Interactive Discussion

Blankenship, D. D., Bentley, C. R., Rooney, S. T., and Alley, R. B.: Seismic measurements reveal a saturated porous till layer beneath an active Antarctic ice stream, Nature, 322, 54–57, doi:10.1038/322054a0, 1986.

Bory, A. J.-M., Biscaye, P. E., Piotrowski, A. M., and Steffensen, J. P.: Regional variability of ice core dust composition and provenance in Greenland, Geochem. Geophy. Geosy., 4, 1107, doi:10.1029/2003GC000627, 2003.

Chen, G.: GPS kinematic positioning for airborne laser altimetry at Long Valley, Ph.D. thesis, Massachussetts Institute of Technology, Cambridge, MA, USA, 1998.

Christianson, K., Jacobel, R. W., Horgan, H. J., Anandakrishnan, S., and Alley, R. B.: Subglacial Lake Whillans – Ice-penetrating radar and GPS observations of a shallow active reservoir beneath a West Antarctic ice stream, Earth Planet. Sc. Lett., 331–332, 237–245, doi:10.1016/j.epsl.2012.03.013, 2012.

Christianson, K., Peters, L. E., Alley, R. B., Anandakrishnan, S., Jacobel, R. W., Riverman, K. L., and Muto, A.: Dilatant till facilitiates streaming ice flow in northeast Greenland, Earth Planet. Sc. Lett., in review, 2014.

Fahnestock, M., Bindschadler, R., Kwok, R., and Jezek, K.: Greenland ice sheet surface properties and ice dynamics from ERS-1 SAR imagery, Science, 262, 1530–1534, doi:10.1126/science.262.5139.1530, 1993.

Fahnestock, M. A., Joughin, I., Scambos, T. A., Kwok, R., Karbill, W. B., and Gogineni, S.: Ice-stream-related patterns of ice flow in the interior of northeast Greenland, J. Geophys. Res., 106, 34035–34045, doi:10.1029/2001JD900194, 2001.

Fischer, H., Wagenbach, D., and Kipfstuhl, J.: Sulfate and nitrate firn concentrations on the Greenland ice sheet 2. Temporal anthropogenic deposition changes, J. Geophys. Res., 103, 21935–21942, doi:10.1029/98JD01886, 1998a.

Fischer, H., Wagenbach, D., and Kipfstuhl, J.: Sulfate and nitrate firn concentrations on the Greenland ice sheet 1. Large-scale geographical deposition changes, J. Geophys. Res., 103, 21927–21934, doi:10.1029/98JD01885, 1998b.

Gkinis, V., Popp, T. J., Blunier, T., Bigler, M., Schüpbach, S., Kettner, E., and Johnsen, S. J.: Water isotopic ratios from a continuously melted ice core sample, Atmos. Meas. Tech., 4, 2531–2542, doi:10.5194/amt-4-2531-2011, 2011.

Gow, A. J.: On the accumulation and seasonal stratification of snow at the South Pole, J. Glaciol., 5, 467–477, 1965.

Title Page

Abstract | Introduction

Conclusions | References

Tables | Figures

◀◀ | ▶▶

◀ | ▶

Back | Close

Full Screen / Esc

Printer-friendly Version

Interactive Discussion

Holland, D. M., Thomas, R. H., De Young, B., Ribergaard, M. H., and Lyberth, B.: Acceleration of Jakobshavn Isbrae triggered by warm subsurface ocean waters, Nat. Geosci., 1, 659–664, doi:10.1038/ngeo316, 2008.

Joughin, I., Fahnestock, M., MacAyeal, D., Bamber, J. L., and Gogineni, P.: Observation and analysis of ice flow in the largest Greenland ice stream, J. Geophys. Res., 106, 34021–34034, doi:10.1029/2001jd900087, 2001.

Joughin, I., Smith, B. E., and Holland, D. M.: Sensitivity of 21st century sea level to ocean-induced thinning of Pine Island Glacier, Antarctica, Geophys. Res. Lett., 37, L20502, doi:10.1029/2010gl044819, 2010.

Joughin, I., Alley, R. B., and Holland, D. M.: Ice-Sheet Response to Oceanic Forcing, Science, 338, 1172–1176, doi:10.1126/science.1226481, 2012a.

Joughin, I., Smith, B. E., Howat, I. M., Floricioiu, D., Alley, R. B., Truffer, M., and Fahnestock, M.: Seasonal to decadal scale variations in the surface velocity of Jakobshavn Isbrae, Greenland: observation and model-based analysis, J. Geophys. Res., 117, F02030, doi:10.1029/2011jf002110, 2012b.

Kamb, B.: Basal Zone of the West Antarctic ice streams and its role in lubrication of their rapid motion, in: The West Antarctic Ice Sheet: Behavior and Environment, edited by: Alley, R. B. and Bindschadler, R. A., Antarctic Research Series, American Geophysical Union, Washington DC, 157–159, 2001.

Keisling, B. A., Christianson, K., Alley, R. B., Peters, L. E., Christian, J. E. M., Anandakrishnan, S., Riverman, K. L., Muto, A., and Jacobel, R. W.: Basal conditions and ice dynamics inferred from radar-derived internal stratigraphy of the Northeast Greenland Ice Stream, Ann. Glaciol., in review, 2014.

Kirchner, J. F. and Bentley, C. R.: RIGGS III: Seismic short-refraction studies using an analytical curve-fitting technique, in: The Ross Ice Shelf: Glaciology and Geophysics, edited by: Bentley, C. R., and Hayes, D. E., Antarctic Research Series, American Geophysical Union, Washington DC, 1990.

Kjær, H. A., Vallelonga, P., Svensson, A., Kristensen, M. E. L., Tibuleac, C., and Bigler, M.: Continuous flow analysis method for determination of dissolved reactive phosphorus in ice cores, Environ. Sci. Technol., 47, 12325–12332, doi:10.1021/es402274z, 2013.

Kohnen, H.: On the relation between seismic velocities and density in firn and ice, Zeitschrift für Geophysik, 38, 925–935, 1972.

Title Page

Abstract | Introduction

Conclusions | References

Tables | Figures

|◄ | ►|

◄ | ►

Back | Close

Full Screen / Esc

Printer-friendly Version

Interactive Discussion

Legrand, M. and Mayewski, P.: Glaciochemistry of Polar ice cores: a review, Rev. Geophys., 35, 219–243, doi:10.1029/96RG03527, 1997.

Legrand, M., De Angelis, M., Staffelbach, T., Neftel, A., and Stauffer, B.: Large perturbations of ammonium and organic acids content in the Summit-Greenland ice core. Fingerprint from forest fires?, Geophys. Res. Lett., 19, 473–475, doi:10.1029/91GL03121, 1992.

Marlon, J. R., Bartlein, P. J., Carcaillet, C., Gavin, D. G., Harrison, S. P., Higuera, P. E., Joos, F., Power, M. J., and Prentice, I. C.: Climate and human influences on global biomass burning over the past two millennia, Nat. Geosci., 1, 697–702, doi:10.1038/ngeo313, 2008.

Moon, T., Joughin, I., Smith, B., and Howat, I.: 21st-century evolution of greenland outlet glacier velocities, Science, 336, 576–578, doi:10.1126/science.1219985, 2012.

Moore, J. C., Mulvaney, R., and Paren, J. G.: Dielectric stratigraphy of ice: a new technique for determining total ionic concentrations in polar ice cores, Geophys. Res. Lett., 16, 1177–1180, doi:10.1029/GL016i010p01177, 1989.

NEEM Community members: Eemian interglacial reconstructed from a Greenland folded ice core, Nature, 493, 489–494, doi:10.1038/nature11789, 2013.

NGRIP members: High-resolution record of Northern Hemisphere climate extending into the last interglacial period, Nature, 431, 147–151, doi:10.1038/nature02805, 2004.

Peters, L. E., Anandakrishnan, S., Alley, R. B., and Smith, A. M.: Extensive storage of basal meltwater in the onset region of a major West Antarctic ice stream, Geology, 35, 251–254, doi:10.1130/G23222A.1, 2007.

Peters, L. E., Anandakrishnan, S., Holland, C. W., Horgan, H. J., Blankenship, D. D., and Voigt, D. E.: Seismic detection of a subglacial lake near the South Pole, Antarctica, Geophys. Res. Lett., 35, L23501, doi:10.1029/2008GL035704, 2008.

Peters, L. E.: A seismic investigation of basal conditions in glaciated regions, Ph.D. thesis, The Pennsylvania State University, USA, 2009.

Petrunin, A. G., Rogozhina, I., Vaughan, A. P. M., Kukkonen, I. T., Kaban, M. K., Koulakov, I., and Thomas, M.: Heat flux variations beneath central Greenland's ice due to anomalously thin lithosphere, Nat. Geosci., 6, 746–750, doi:10.1038/ngeo1898, 2013.

Pfeffer, W. T., Harper, J. T., and O'Neel, S.: Kinematic constraints on glacier contributions to 21st-century sea-level rise, Science, 321, 1340–1343, doi:10.1126/science.1159099, 2008.

Reeh, N., S. Johnsen, J., and Dahl-Jensen, D.: Dating the Dye 3 deep ice core by flow model calculations, in: Greenland Ice Cores: Geophysics, Geochemistry and the Environment, Geophysical Monograph 33, American Geophysical Union, Washington DC, USA, 1985.

Title Page

Abstract | Introduction

Conclusions | References

Tables | Figures

|◄ | ►|

◄ | ►

Back | Close

Full Screen / Esc

Printer-friendly Version

Interactive Discussion

Rignot, E., Velicogna, I., van den Broeke, M. R., Monaghan, A., and Lenaerts, J. T. M.: Acceleration of the contribution of the Greenland and Antarctic ice sheets to sea level rise, Geophys. Res. Lett., 38, L05503, doi:10.1029/2011gl046583, 2011.

Straneo, F., Sutherland, D. A., Holland, D., Gladish, C., Hamilton, G., Johnson, H., Rignot, E., Xu, Y., and Koppes, M.: Characteristics of ocean waters reaching Greenland's glaciers, Ann. Glaciol., 53, 202–210, doi:10.3189/2012AoG60A059, 2012.

van den Broeke, M., Bamber, J., Ettema, J., Rignot, E., Schrama, E., van de Berg, W. J., van Meijgaard, E., Velicogna, I., and Wouters, B.: Partitioning recent greenland mass loss, Science, 326, 984–986, doi:10.1126/science.1178176, 2009.

Welch, B. C. and Jacobel, R. W.: Analysis of deep-penetrating radar surveys of West Antarctica, US-ITASE 2001, Geophys. Res. Lett., 30, 1444, doi:10.1029/2003GL017210, 2003.

Welch, B. C., Jacobel, R. W., and Arcone, S.: First results from radar profiles collected along the US-ITASE traverse from Taylor Dome to South Pole (2006–2008), Ann. Glaciol., 50, 35–41, doi:10.3189/172756409789097496, 2009.

Winstrup, M., Svensson, A. M., Rasmussen, S. O., Winther, O., Steig, E. J., and Axelrod, A. E.: An automated approach for annual layer counting in ice cores, Clim. Past, 8, 1881–1895, doi:10.5194/cp-8-1881-2012, 2012.

Wolff, E. W., Chappellaz, J., Blunier, T., Rasmussen, S. O., and Svensson, A.: Millennial-scale variability during the last glacial: the ice core record, Quaternary Sci. Rev., 29, 2828–2838, doi:10.1016/j.quascirev.2009.10.013, 2010.

Wouters, B., Bamber, J. L., van den Broeke, M. R., Lenaerts, J. T. M., and Sasgen, I.: Limits in detecting acceleration of ice sheet mass loss due to climate variability, Nat. Geosci., 6, 613–616, doi:10.1038/ngeo1874, 2013.

Yin, J.: Century to multi-century sea level rise projections from CMIP5 models, Geophys. Res. Lett., 39, L17709, doi:10.1029/2012gl052947, 2012.

Initial results from Northeast Greenland Ice Stream (NEGIS)

P. Vallelonga et al.

Title Page

Abstract | Introduction

Conclusions | References

Tables | Figures

◄ | ►

◄ | ►

Back | Close

Full Screen / Esc

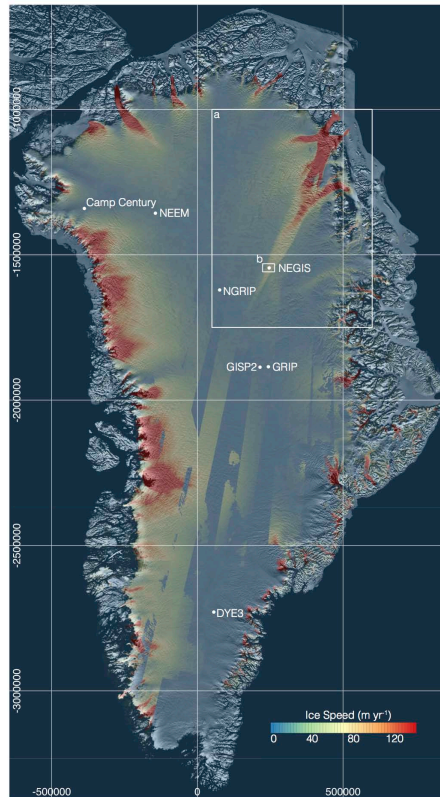Printer-friendly Version

Interactive Discussion

Fig. 1. Locations of Greenland ice core drilling sites and the Northeast Greenland Ice Stream (NEGIS), NEEM, NorthGRIP (NGRIP), GRIP, GISP2, DYE3, and Camp Century. Velocities from interferometric synthetic aperture radar data are shown in color (Joughin et al., 2010). Background is MODIS imagery (T. Haran, personal communication, 2012). The white boxes denote areas shown in Figs. 2 and 3. Projection is polar stereographic relative to WGS84 ellipsoid with central meridian at 45° W and standard parallel at 70° N.
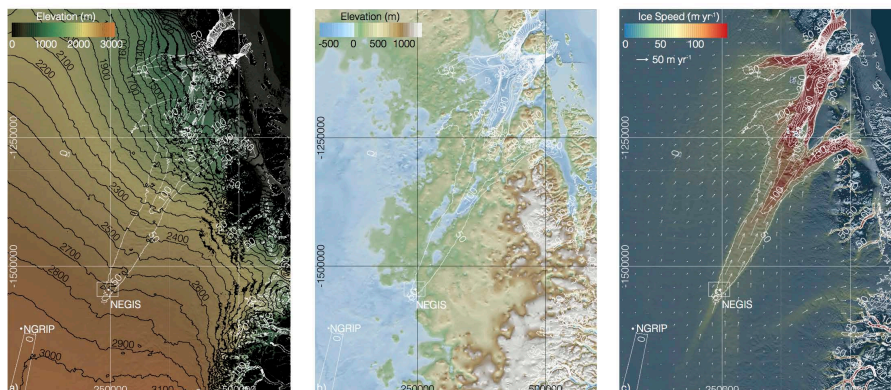
Fig. 2. (a) Surface elevation, **(b)** bedrock elevation, and **(c)** ice velocity of northeast Greenland. Background imagery is MODIS (T. Haran, personal communication, 2012). Bed elevation is from Bamber et al. (2013). Velocities are derived from interferometric synthetic aperature radar data (Joughin et al., 2010). Surface elevation (black) and ice speed (white) contour intervals are 100 m and 50 m yr^{-1}, respectively. White box denotes area shown in Fig. 3. Projection is polar stereographic relative to WGS84 ellipsoid with central meridian at 45° W and standard parallel at 70° N. Surface elevation is relative to WGS84 ellipsoid and bed elevation/bathymetry is relative to EIGEN-GL04C geoid.
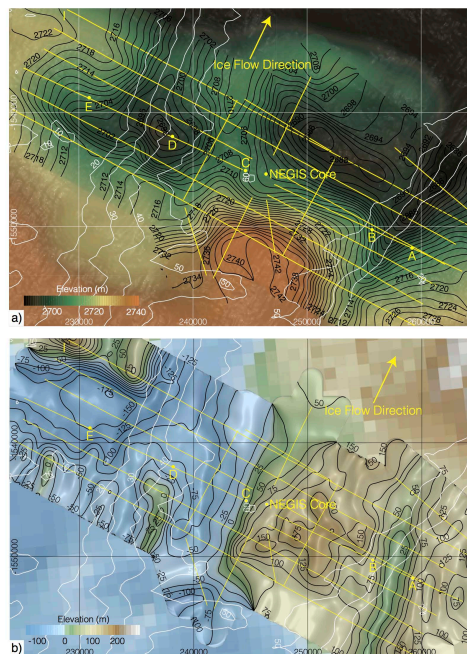
Fig. 3. (a) Surface and **(b)** bedrock elevation of NEGIS interpolated from kinematic GPS profiles and RES profiles (yellow lines), respectively. Seismic sites are labelled A–E. Radar profile I–II is shown in Fig. 4. The shallow core (NEGIS core) is in the center of the geophysical survey grid (yellow lines). In **(a)** black contours (1 m interval) show surface elevation (relative to WGS84 ellipsoid) and in **(b)** they show bed elevation (25 m interval). White contours show ice surface speed ($10 \, \text{m yr}^{-1}$ interval from interferometric synthetic aperture radar data (Joughin et al., 2010). Background is MODIS imagery with Lambertian radiance applied (T. Haran, personal communication, 2012) in **(a)**. Background bed topography is from Bamber et al. (2013). Projection is polar stereographic relative to WGS84 ellipsoid with central meridian at 45° W and standard parallel at 70° N.
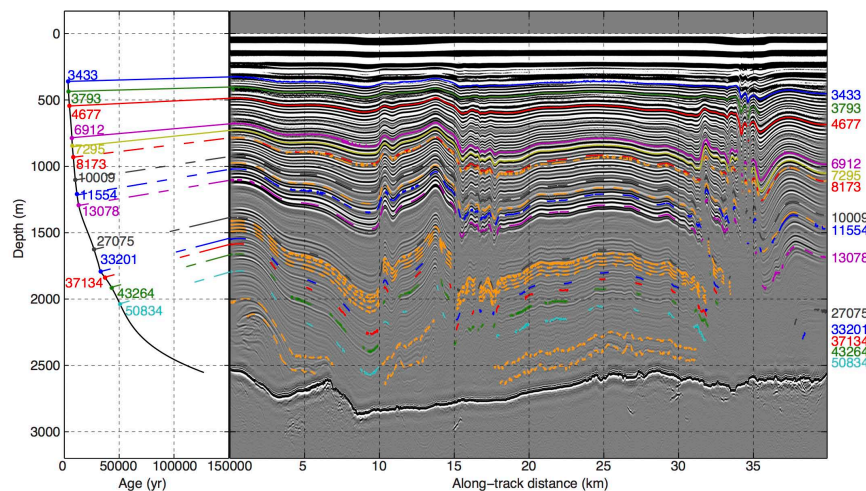
Fig. 4. Profile I-II (from Fig. 3) with dated internal layers. Age scale is assigned by tracing internal layers dated in the NGRIP core from NGRIP to NEGIS in airborne radio-echo sounding (RES).
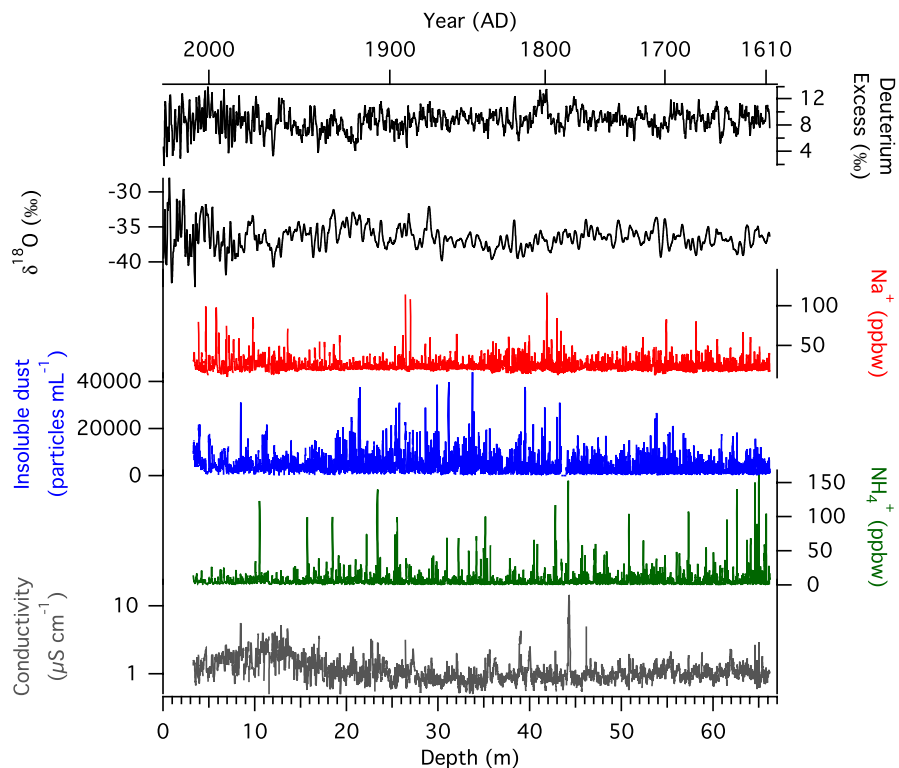
Fig. 5. Stable water isotopologues and chemical impurities determined in the NEGIS firn core. δ^{18}O and deuterium excess were determined in discretely cut ice sampled at 5 cm resolution while the impurities were determined from continuous flow analysis measurements.

Title Page

Abstract | Introduction

Conclusions | References

Tables | Figures

|◀ | ▶|

◀ | ▶

Back | Close
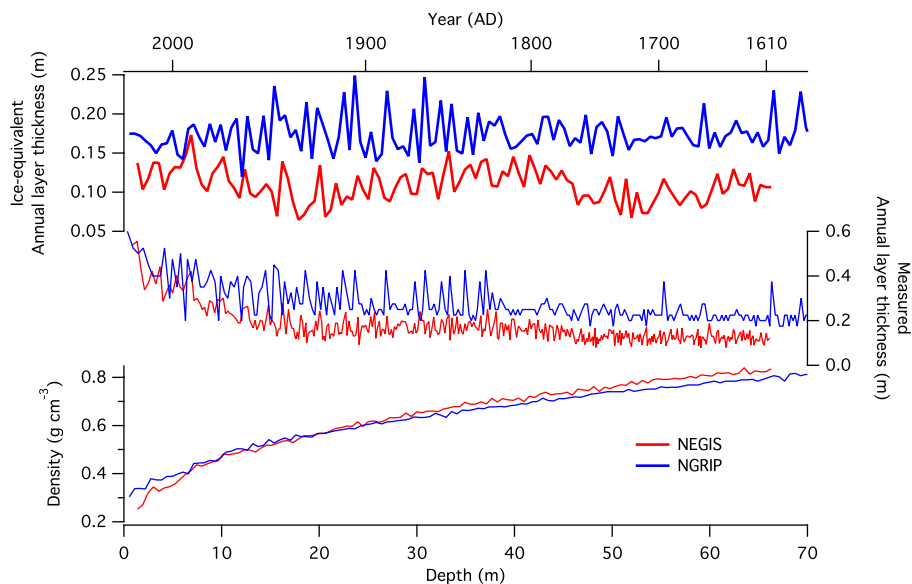
Full Screen / Esc

Printer-friendly Version

Interactive Discussion

Fig. 6. Annual layer thickness and density profiles for the NEGIS firn core and the upper 70 m of the NGRIP ice core.
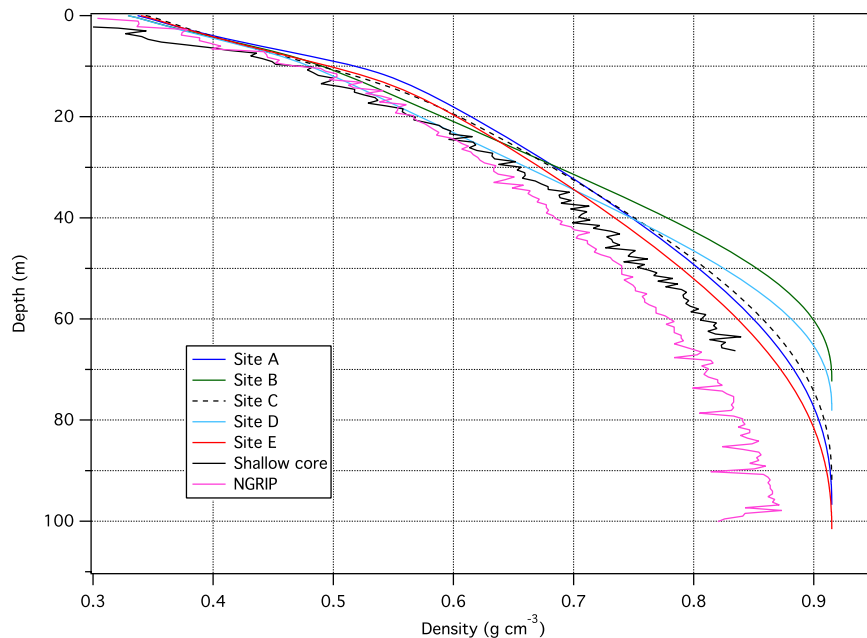
Fig. 7. Firn density profiles determined from seismic shallow refraction data at sites A-E (Fig. 3). Note that density in all profiles approaches ice density ($917\,\mathrm{kg\,m^{-3}}$) by $\sim 90\,\mathrm{m}$, but that the sites in the shear margins (B and D) exhibit higher densification rates. For comparison, the directly measured densities of the NEGIS shallow core (black line) and NGRIP ice core (pink line) are also plotted. Differences between measured and derived density curves are consistent with those expected from the seismic analysis (Kohnen, 1972; Kirchner and Bentley, 1990).

Title Page

Abstract | Introduction

Conclusions | References

Tables | Figures

◄ | ►

◄ | ►

Back | Close

Full Screen / Esc

Printer-friendly Version

Interactive Discussion